

# Analysis of immune-related loci identifies 48 new susceptibility variants for multiple sclerosis

International Multiple Sclerosis Genetics Consortium (IMSGC)\*

**Using the ImmunoChip custom genotyping array, we analyzed 14,498 subjects with multiple sclerosis and 24,091 healthy controls for 161,311 autosomal variants and identified 135 potentially associated regions ( $P < 1.0 \times 10^{-4}$ ). In a replication phase, we combined these data with previous genome-wide association study (GWAS) data from an independent 14,802 subjects with multiple sclerosis and 26,703 healthy controls. In these 80,094 individuals of European ancestry, we identified 48 new susceptibility variants ( $P < 5.0 \times 10^{-8}$ ), 3 of which we found after conditioning on previously identified variants. Thus, there are now 110 established multiple sclerosis risk variants at 103 discrete loci outside of the major histocompatibility complex. With high-resolution Bayesian fine mapping, we identified five regions where one variant accounted for more than 50% of the posterior probability of association. This study enhances the catalog of multiple sclerosis risk variants and illustrates the value of fine mapping in the resolution of GWAS signals.**

Multiple sclerosis (MIM 126200) is an inflammatory demyelinating disorder of the central nervous system that is a common cause of chronic neurological disability<sup>1,2</sup>. It shows greatest prevalence among individuals of northern European ancestry<sup>3</sup> and is moderately heritable<sup>4</sup>, with a sibling relative recurrence risk ( $\lambda_s$ ) of  $\sim 6.3$  (ref. 5). Aside from early success in demonstrating the important effects exerted by variants in the human leukocyte antigen (HLA) genes from the major histocompatibility complex (MHC)<sup>6</sup>, there was little progress in unraveling the genetic architecture underlying susceptibility to multiple sclerosis before the advent of GWAS technology. Over the last decade, our consortium has performed several GWAS and meta-analyses in large cohorts<sup>7–10</sup>, cumulatively identifying more than 50 non-MHC susceptibility alleles. As in other complex diseases, available data suggest that many additional susceptibility alleles remain to be identified<sup>11</sup>.

The striking overlap in the genetic architectures underlying susceptibility to multiple autoimmune diseases<sup>9,10,12,13</sup> prompted the collaborative construction of the ImmunoChip (see **Supplementary Figs. 1 and 2** and the **Supplementary Note** for details on IMSGC-nominated content), an efficient genotyping platform designed to deeply interrogate 184 non-MHC loci with genome-wide significant associations to at least 1 autoimmune disease and to provide lighter coverage of

other genomic regions with suggestive evidence of association<sup>14</sup>. Here we report a large-scale effort that leverages the ImmunoChip to detect association with multiple sclerosis susceptibility and to refine these associations via Bayesian fine mapping.

After performing stringent quality control, we report genotypes for 28,487 individuals of European ancestry (14,498 subjects with multiple sclerosis and 13,989 healthy controls) that are independent of the genotypes examined in previous GWAS efforts. We supplemented these data with genotypes from 10,102 independent control subjects provided by the International Inflammatory Bowel Disease Genetics Consortium (IIBDGC)<sup>15</sup>, bringing the total number of subjects to 38,589 (14,498 subjects with multiple sclerosis and 24,091 healthy controls). We performed variant-level quality control, population outlier identification and subsequent case-control analysis in 11 country-organized strata. To account for within-stratum population stratification, we used the first five principal components as covariates in the association analysis. Per-stratum odds ratio (OR) and respective standard error (s.e.) estimates were then combined with an inverse variance meta-analysis under a fixed-effects model. In total, we tested 161,311 autosomal variants that passed quality control in at least 2 of the 11 strata (Online Methods). A Circos plot<sup>16</sup> summarizing the results from this discovery phase analysis is shown in **Figure 1**.

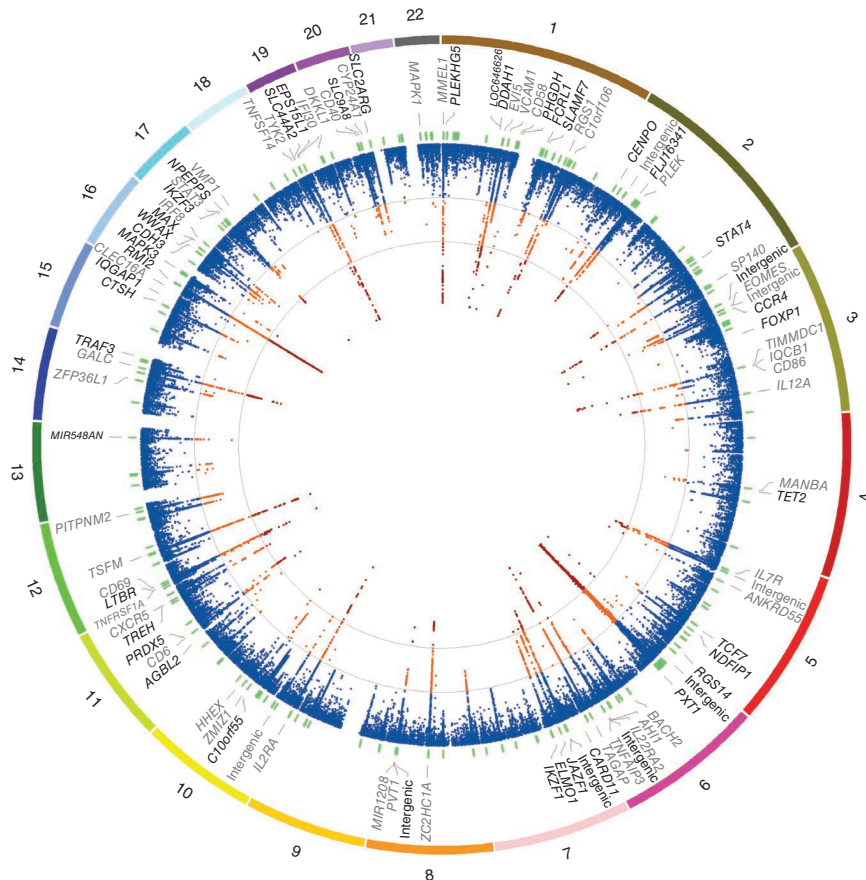
We defined an *a priori* significance threshold of  $P < 1 \times 10^{-4}$  for the discovery phase and identified 135 statistically independent primary association signals, comprising 67 in the designated fine-mapping regions and 68 in less densely covered regions selected for deep replication of earlier GWAS signals. Using forward stepwise logistic regression, we identified a second statistically independent signal in 13 of these regions (secondary signals) and a third statistically independent signal in 2 regions (tertiary signals). A total of 48 of the 150 statistically independent association signals (**Supplementary Table 1**) reached genome-wide significance of  $P < 5 \times 10^{-8}$  in the discovery phase alone. Next, we replicated our findings in 14,802 subjects with multiple sclerosis and 26,703 healthy controls with available GWAS data imputed using the 1000 Genomes Project European phase I (a) panel (Online Methods). Finally, we performed a joint analysis of the discovery and replication phases.

We identified 97 statistically independent SNPs meeting replication criteria (replication  $P < 0.05$ , joint  $P < 5 \times 10^{-8}$  and joint  $P < \text{discovery } P$ ), comprising 93 primary signals (**Supplementary Figs. 3–95**) and 4 secondary signals. Of these signals, 48 are new

\*Full lists of authors and affiliations appear at the end of the paper.

Received 24 April; accepted 3 September; published online 29 September 2013; doi:10.1038/ng.2770

**Figure 1** Discovery phase results. Circos plot showing primary association analysis of 161,311 autosomal variants in the discovery phase (14,498 cases and 24,091 healthy controls). The outermost track shows the numbered autosomal chromosomes. The second track indicates the gene closest to the most associated SNP meeting all replication criteria. Previously identified associations are indicated in gray. The third track indicates the physical position of the 184 fine-mapping intervals (green). The innermost track indicates  $-\log(P)$  (two-sided) for each SNP (scaled from 0–12, which truncates the signal in several regions; **Supplementary Table 1**). Additionally, contour lines are given at the *a priori* discovery ( $-\log(P) = 4$ ) and genome-wide significance ( $-\log(P) = 7.3$ ) thresholds. Orange indicates  $-\log(P) \geq 4$  and  $< 7.3$ , and red indicates  $-\log(P) \geq 7.3$ . Details of the full discovery phase results can be found in ImmunoBase (see URLs).



to multiple sclerosis (**Table 1**), and 49 correspond to previously identified susceptibility loci for multiple sclerosis (**Table 2**). An additional 11 independent SNPs showed suggestive evidence of association (joint  $P < 1 \times 10^{-6}$ ) (**Supplementary Table 2**).

The strongest newly associated SNP, rs12087340 (joint  $P = 1.1 \times 10^{-20}$ ; OR = 1.21), lies between *BCL10* (encoding B cell CLL/lymphoma 10) and *DDAH1* (encoding dimethylarginine dimethylaminohydrolase 1). The protein encoded by *BCL10* contains a caspase recruitment domain (CARD) and has been shown to activate nuclear factor (NF)- $\kappa$ B signaling<sup>17</sup>. This signaling molecule has an important role in controlling gene expression in inflammation, immunity, cell proliferation and apoptosis. It has been pursued as a potential therapeutic target for multiple sclerosis<sup>18</sup>. *BCL10* is also reported to interact with other CARD domain-containing proteins, including *CARD11* (ref. 19). We additionally identified a new association for rs1843938 (joint  $P = 1.2 \times 10^{-10}$ ; OR = 1.08), which is only 30 kb away from *CARD11*.

One newly associated SNP, rs2288904 (joint  $P = 1.6 \times 10^{-11}$ ; OR = 1.10), was found within an exon, representing a missense variant in *SLC44A2* (encoding solute carrier family 44, member 2). Notably, this variant is also reported as a monocyte-specific *cis*-acting expression quantitative trait locus (eQTL) for the antisense transcript of the nearby *ILF3* gene (encoding interleukin enhancer-binding factor 3)<sup>20</sup>. The *ILF3* protein was first discovered as a subunit of a nuclear factor found in activated T cells, which is required for T cell expression of *IL2*, an important molecule that regulates many aspects of inflammation.

Of the 49 previously identified risk loci<sup>9,10,21</sup>, 37 are in designated fine-mapping regions, and 23 of these 37 signals were localized to a single gene on the basis of genomic position (**Supplementary Table 3**). Although proximity does not necessarily indicate that these genes are functionally relevant, this observation nevertheless emphasizes the usefulness of dense mapping in localizing signals from a genome-wide screen. Our ImmunoChip analysis furthers the understanding of previously proposed secondary signals at three loci (**Supplementary Tables 4–6** and **Supplementary Note**); in particular, we showed that the effects of two previously proposed independent associations at the *IL2RA* locus<sup>7,22</sup> are driven by a single variant, rs2104286.

In an effort to define the functionally relevant variants underlying these associations, we further studied the regions surrounding the 97 associated SNPs using both Bayesian and frequentist approaches in 6,356 subjects with multiple sclerosis and 9,617 healthy controls from the UK (Online Methods)<sup>23</sup>. As determined by examining imputation quality, fine mapping was possible in 68 regions (**Supplementary Table 7**), including 66 of 93 primary (**Fig. 2a**) and 2 of 4 secondary signals. Eight of the 68 regions were fine mapped to high resolution (**Fig. 2b**, **Table 3** and **Supplementary Fig. 96**). One-third of the variants identified in these eight regions were imputed, indicating the value of imputation, even with dense genotyping coverage.

To assess whether functional annotation<sup>24</sup> provides clues about the molecular mechanisms associated with genetic risk, we considered the relationship of variants to annotated coding and regulatory features in these eight regions. Although we found no variants with missense or nonsense effects, there was a notable enrichment for variants with functional effects, including one variant known to affect splicing<sup>25</sup>, three variants known to correlate with RNA or serum protein levels<sup>22,26,27</sup> and several variants overlapping transcription factor binding sites and DNase I hypersensitive sites<sup>28,29</sup>. Four of the 18 variants in the fine-mapped regions are within conserved regions (GERP > 2)<sup>30</sup>. The overall lack of functional annotation likely reflects the limited repertoire of reference expression and epigenomic profiles and suggests that the function of the variants may be specific to cell type or cell state, as has been reported for many eQTLs in immune cell types<sup>20</sup>.

To determine the Gene Ontology (GO) processes of the 97 associated variants, we used MetaCore from Thomson Reuters (Online Methods). We found that the majority of the 97 variants lie within 50 kb of genes having immunological function. Of the 86 unique genes

**Table 1 Results for 48 new non-MHC variants associated with multiple sclerosis at a genome-wide significance level**

SNP	Chr.	Position <sup>a</sup>	RA	Discovery			Replication			Joint		Gene <sup>b</sup>	Function
				RAF	<i>P</i>	OR	RAF	<i>P</i>	OR	<i>P</i>	OR		
rs3007421	1	6530189	A	0.12	9.6 × 10 <sup>-7</sup>	1.12	0.13	8.8 × 10 <sup>-5</sup>	1.10	4.7 × 10 <sup>-10</sup>	1.11	<i>PLEKHG5</i>	Intronic
rs12087340	1	85746993	A	0.09	5.1 × 10 <sup>-12</sup>	1.22	0.09	2.9 × 10 <sup>-10</sup>	1.20	1.1 × 10 <sup>-20</sup>	1.21	<i>BCL10</i>	Intergenic
rs11587876	1	85915183	A	0.79	8.4 × 10 <sup>-8</sup>	1.12	0.81	2.9 × 10 <sup>-3</sup>	1.06	4.4 × 10 <sup>-9</sup>	1.09	<i>DDAH1</i>	Intronic
rs666930	1	120258970	G	0.53	7.5 × 10 <sup>-8</sup>	1.09	0.53	1.3 × 10 <sup>-5</sup>	1.07	6.0 × 10 <sup>-12</sup>	1.08	<i>PHGDH</i>	Intronic
rs2050568	1	157770241	G	0.53	1.3 × 10 <sup>-6</sup>	1.08	0.54	2.3 × 10 <sup>-5</sup>	1.07	1.5 × 10 <sup>-10</sup>	1.08	<i>FCRL1</i>	Intronic
rs35967351	1	160711804	A	0.67	1.7 × 10 <sup>-6</sup>	1.09	0.68	5.9 × 10 <sup>-6</sup>	1.09	4.4 × 10 <sup>-11</sup>	1.09	<i>SLAMF7</i>	Intronic
rs4665719	2	25017860	G	0.25	6.8 × 10 <sup>-6</sup>	1.09	0.25	1.1 × 10 <sup>-4</sup>	1.08	3.1 × 10 <sup>-9</sup>	1.08	<i>CENPO</i>	Intronic
rs842639	2	61095245	A	0.65	1.7 × 10 <sup>-9</sup>	1.11	0.67	1.4 × 10 <sup>-6</sup>	1.09	2.0 × 10 <sup>-14</sup>	1.10	<i>FLJ16341</i>	Noncoding RNA
rs9967792	2	191974435	G	0.62	1.8 × 10 <sup>-9</sup>	1.11	0.64	1.2 × 10 <sup>-4</sup>	1.07	3.5 × 10 <sup>-12</sup>	1.09	<i>STAT4</i>	Intronic
rs11719975	3	18785585	C	0.27	5.4 × 10 <sup>-6</sup>	1.09	0.28	4.1 × 10 <sup>-4</sup>	1.07	1.1 × 10 <sup>-8</sup>	1.08		Intergenic
rs4679081	3	33013483	G	0.52	1.2 × 10 <sup>-5</sup>	1.08	0.55	3.7 × 10 <sup>-4</sup>	1.07	2.2 × 10 <sup>-9</sup>	1.07	<i>CCR4</i>	Intergenic
rs9828629	3	71530346	G	0.62	5.5 × 10 <sup>-6</sup>	1.08	0.64	8.5 × 10 <sup>-6</sup>	1.08	1.9 × 10 <sup>-10</sup>	1.08	<i>FOXPI</i>	Intronic
rs2726518	4	106173199	C	0.55	1.2 × 10 <sup>-5</sup>	1.09	0.58	4.7 × 10 <sup>-4</sup>	1.06	3.9 × 10 <sup>-8</sup>	1.07	<i>TET2</i>	Intronic
rs756699	5	133446575	A	0.87	3.0 × 10 <sup>-6</sup>	1.12	0.88	6.5 × 10 <sup>-6</sup>	1.11	8.8 × 10 <sup>-11</sup>	1.12	<i>TCF7</i>	Intergenic
None <sup>c</sup>	5	141506564	C	0.61	6.0 × 10 <sup>-5</sup>	1.07	0.62	1.5 × 10 <sup>-5</sup>	1.08	3.6 × 10 <sup>-9</sup>	1.07	<i>NDFIP1</i>	Intronic
rs4976646	5	176788570	G	0.34	1.0 × 10 <sup>-12</sup>	1.13	0.36	5.0 × 10 <sup>-7</sup>	1.10	4.4 × 10 <sup>-18</sup>	1.12	<i>RGS14</i>	Intronic
rs17119	6	14719496	A	0.81	1.9 × 10 <sup>-6</sup>	1.11	0.80	1.2 × 10 <sup>-5</sup>	1.10	1.0 × 10 <sup>-10</sup>	1.10		Intergenic
rs941816	6	36375304	G	0.18	4.5 × 10 <sup>-9</sup>	1.13	0.20	8.3 × 10 <sup>-5</sup>	1.08	3.9 × 10 <sup>-12</sup>	1.11	<i>PXT1</i>	Intronic
rs1843938	7	3113034	A	0.44	2.2 × 10 <sup>-6</sup>	1.08	0.44	1.1 × 10 <sup>-5</sup>	1.08	1.2 × 10 <sup>-10</sup>	1.08	<i>CARD11</i>	Intergenic
rs706015	7	27014988	C	0.18	1.3 × 10 <sup>-9</sup>	1.14	0.18	9.9 × 10 <sup>-3</sup>	1.06	1.1 × 10 <sup>-9</sup>	1.10		Intergenic
rs917116	7	28172739	C	0.20	2.1 × 10 <sup>-8</sup>	1.12	0.21	5.8 × 10 <sup>-3</sup>	1.06	3.3 × 10 <sup>-9</sup>	1.09	<i>JAZF1</i>	Intronic
rs60600003	7	37382465	C	0.10	2.5 × 10 <sup>-8</sup>	1.16	0.10	4.2 × 10 <sup>-7</sup>	1.14	6.0 × 10 <sup>-14</sup>	1.15	<i>ELMO1</i>	Intronic
rs201847125 <sup>d</sup>	7	50325567	G	0.70	2.9 × 10 <sup>-8</sup>	1.11	0.70	6.7 × 10 <sup>-5</sup>	1.09	1.2 × 10 <sup>-11</sup>	1.10	<i>IKZF1</i>	Intergenic
rs2456449	8	128192981	G	0.36	2.2 × 10 <sup>-8</sup>	1.10	0.37	3.8 × 10 <sup>-3</sup>	1.05	1.8 × 10 <sup>-9</sup>	1.08		Intergenic
rs793108	10	31415106	A	0.50	5.6 × 10 <sup>-8</sup>	1.09	0.51	1.8 × 10 <sup>-5</sup>	1.07	6.1 × 10 <sup>-12</sup>	1.08		Intergenic
rs2688608	10	75658349	A	0.55	6.4 × 10 <sup>-5</sup>	1.07	0.56	2.0 × 10 <sup>-4</sup>	1.06	4.6 × 10 <sup>-8</sup>	1.07	<i>C10orf55</i>	Intergenic
rs7120737	11	47702395	G	0.15	7.6 × 10 <sup>-8</sup>	1.13	0.15	1.0 × 10 <sup>-3</sup>	1.08	1.0 × 10 <sup>-9</sup>	1.10	<i>AGBL2</i>	Intronic
rs694739	11	64097233	A	0.62	1.3 × 10 <sup>-5</sup>	1.08	0.62	3.8 × 10 <sup>-5</sup>	1.07	2.0 × 10 <sup>-9</sup>	1.07	<i>PRDX5</i>	Intergenic
rs9736016	11	118724894	T	0.63	2.2 × 10 <sup>-8</sup>	1.10	0.63	2.6 × 10 <sup>-8</sup>	1.10	3.0 × 10 <sup>-15</sup>	1.10	<i>CXCR5</i>	Intergenic
rs12296430	12	6503500	C	0.19	3.6 × 10 <sup>-10</sup>	1.14	0.21	1.7 × 10 <sup>-5</sup>	1.09	7.2 × 10 <sup>-14</sup>	1.12	<i>LTBR</i>	Intergenic
rs4772201	13	100086259	A	0.82	1.7 × 10 <sup>-7</sup>	1.12	0.83	1.1 × 10 <sup>-4</sup>	1.09	1.3 × 10 <sup>-10</sup>	1.10	<i>MIR548AN</i>	Intergenic
rs12148050	14	103263788	A	0.35	1.5 × 10 <sup>-5</sup>	1.08	0.36	4.3 × 10 <sup>-9</sup>	1.10	5.1 × 10 <sup>-13</sup>	1.09	<i>TRAF3</i>	Intronic
rs59772922	15	79207466	A	0.83	4.0 × 10 <sup>-6</sup>	1.11	0.83	5.4 × 10 <sup>-4</sup>	1.08	1.2 × 10 <sup>-8</sup>	1.09	<i>CTSH</i>	Intergenic
rs8042861	15	90977333	A	0.44	9.8 × 10 <sup>-7</sup>	1.08	0.45	3.4 × 10 <sup>-4</sup>	1.06	2.2 × 10 <sup>-9</sup>	1.07	<i>IQGAP1</i>	Intronic
rs6498184	16	11435990	G	0.81	2.1 × 10 <sup>-10</sup>	1.15	0.82	6.5 × 10 <sup>-9</sup>	1.14	7.4 × 10 <sup>-18</sup>	1.15	<i>RMI2</i>	Intergenic
rs7204270 <sup>e</sup>	16	30156963	G	0.50	9.3 × 10 <sup>-8</sup>	1.09	0.49	3.7 × 10 <sup>-5</sup>	1.08	1.6 × 10 <sup>-11</sup>	1.09	<i>MAPK3</i>	Intergenic
rs1886700	16	68685905	A	0.14	8.8 × 10 <sup>-6</sup>	1.11	0.14	3.2 × 10 <sup>-4</sup>	1.08	1.3 × 10 <sup>-8</sup>	1.10	<i>CDH3</i>	Intronic
rs12149527	16	79110596	A	0.47	1.7 × 10 <sup>-6</sup>	1.08	0.47	4.3 × 10 <sup>-6</sup>	1.08	3.3 × 10 <sup>-11</sup>	1.08	<i>WWOX</i>	Intronic
rs7196953	16	79649394	A	0.29	2.6 × 10 <sup>-5</sup>	1.08	0.30	7.9 × 10 <sup>-7</sup>	1.09	1.0 × 10 <sup>-10</sup>	1.09	<i>MAF</i>	Intergenic
rs12946510	17	37912377	A	0.47	8.5 × 10 <sup>-6</sup>	1.08	0.48	8.0 × 10 <sup>-5</sup>	1.07	2.9 × 10 <sup>-9</sup>	1.07	<i>IKZF3</i>	Intergenic
rs4794058	17	45597098	A	0.50	1.6 × 10 <sup>-5</sup>	1.07	0.52	3.5 × 10 <sup>-10</sup>	1.11	1.0 × 10 <sup>-13</sup>	1.09	<i>NPEPPS</i>	Intergenic
rs2288904	19	10742170	G	0.77	9.6 × 10 <sup>-10</sup>	1.14	0.78	5.4 × 10 <sup>-4</sup>	1.07	1.6 × 10 <sup>-11</sup>	1.10	<i>SLC44A2</i>	Exonic
rs1870071	19	16505106	G	0.29	5.7 × 10 <sup>-10</sup>	1.12	0.30	4.6 × 10 <sup>-7</sup>	1.09	2.0 × 10 <sup>-15</sup>	1.10	<i>EPS15L1</i>	Intronic
rs17785991	20	48438761	A	0.35	6.4 × 10 <sup>-7</sup>	1.09	0.34	5.9 × 10 <sup>-3</sup>	1.05	4.2 × 10 <sup>-8</sup>	1.07	<i>SLC9A8</i>	Intronic
rs2256814	20	62373983	A	0.19	8.3 × 10 <sup>-7</sup>	1.11	0.21	6.4 × 10 <sup>-4</sup>	1.08	3.5 × 10 <sup>-9</sup>	1.09	<i>SLC2A4RG</i>	Intronic
<b>Secondary</b>													
rs7769192 <sup>f</sup>	6	137962655	G	0.55	1.3 × 10 <sup>-5</sup>	1.08	0.54	5.1 × 10 <sup>-5</sup>	1.07	3.3 × 10 <sup>-9</sup>	1.08		Intergenic
rs533646 <sup>g</sup>	11	118566746	G	0.68	3.6 × 10 <sup>-7</sup>	1.10	0.68	3.9 × 10 <sup>-5</sup>	1.08	7.6 × 10 <sup>-11</sup>	1.09	<i>TREH</i>	Intergenic
rs4780346 <sup>h</sup>	16	11288806	A	0.23	6.8 × 10 <sup>-6</sup>	1.09	0.25	1.5 × 10 <sup>-5</sup>	1.09	4.4 × 10 <sup>-10</sup>	1.09	<i>CLEC16A</i>	Intergenic

All listed signals had discovery  $P \leq 1.0 \times 10^{-4}$ , replication  $P \leq 5.0 \times 10^{-2}$  and joint  $P \leq 5.0 \times 10^{-8}$ . All *P* values are two-sided. Chr., chromosome; RA, risk allele; RAF, risk allele frequency.

<sup>a</sup>Position is based on hg19 and dbSNP Build 137. <sup>b</sup>The nearest gene is listed if it lies within 50 kb of the signal. Bold font indicates genes that are part of the GO immune system process. <sup>c</sup>Proxy SNP rs1036207 ( $r^2 = 0.99$ ) was used in replication. <sup>d</sup>Proxy SNP rs716719 ( $r^2 = 1.00$ ) was used in replication. <sup>e</sup>The primary SNP was rs11865086 ( $P = 1.77 \times 10^{-8}$ ) in the discovery phase, but this SNP (or a good proxy) was not available in replication, so the next best discovery SNP was used. <sup>f</sup>*P* values and OR values shown are after conditioning on rs67297943 (Table 2). <sup>g</sup>*P* values and OR values shown are after conditioning on rs9736016 (Table 2). <sup>h</sup>*P* values and OR values shown are after conditioning on rs12927355 (Table 2).

represented, 35 are linked to the GO immune system process (Tables 1 and 2). We did not see substantial over- or under-representation of certain GO processes when comparing the newly discovered and previously identified loci, but this may represent a limitation of the ImmunoChip in targeting genomic loci enriched for immunologically active genes, as more subtle distinctions between such loci might not be adequately captured by broad annotations such as GO processes.

Finally, we explored the overlap between our findings and those in other autoimmune diseases with reported ImmunoChip analyses. We calculated the percentage of multiple sclerosis signals (110 non-MHC; Supplementary Table 8) overlapping with those of other autoimmune diseases by requiring  $r^2 \geq 0.8$  between the best variants reported in each study using SNAP<sup>31</sup>. In total, we found that ~22% of our signals overlapped at least one other autoimmune disease signal.

**Table 2 Results for 49 known non-MHC variants associated with multiple sclerosis at genome-wide significance**

SNP	Chr.	Position <sup>a</sup>	RA	Discovery			Replication			Joint		Gene <sup>b</sup>	Function
				RAF	<i>P</i>	OR	RAF	<i>P</i>	OR	<i>P</i>	OR		
rs3748817	1	2525665	A	0.64	$1.3 \times 10^{-12}$	1.14	0.65	$1.2 \times 10^{-15}$	1.15	$1.3 \times 10^{-26}$	1.14	<i>MMEL1</i>	Intronic
rs41286801	1	92975464	A	0.14	$7.9 \times 10^{-16}$	1.20	0.16	$2.1 \times 10^{-12}$	1.17	$1.4 \times 10^{-26}$	1.19	<i>EVI5</i>	3' UTR
rs7552544 <sup>c</sup>	1	101240893	A	0.56	$3.7 \times 10^{-6}$	1.08	0.43	$3.3 \times 10^{-12}$	1.12	$1.9 \times 10^{-16}$	1.10	<i>VCAM1</i>	Intergenic
rs6677309	1	117080166	A	0.88	$1.5 \times 10^{-28}$	1.34	0.88	$4.1 \times 10^{-16}$	1.24	$5.4 \times 10^{-42}$	1.29	<i>CD58</i>	Intronic
rs1359062	1	192541472	C	0.82	$1.8 \times 10^{-13}$	1.18	0.83	$2.1 \times 10^{-8}$	1.13	$4.8 \times 10^{-20}$	1.15	<i>RGS1</i>	Intergenic
rs55838263	1	200874728	A	0.71	$1.4 \times 10^{-9}$	1.12	0.71	$3.9 \times 10^{-11}$	1.13	$4.0 \times 10^{-19}$	1.13	<i>C1orf106</i>	Intronic
rs2163226	2	43361256	A	0.71	$7.0 \times 10^{-8}$	1.10	0.73	$3.8 \times 10^{-10}$	1.14	$2.1 \times 10^{-16}$	1.12		Intergenic
rs7595717	2	68587477	A	0.26	$3.3 \times 10^{-7}$	1.10	0.27	$6.8 \times 10^{-8}$	1.10	$1.2 \times 10^{-13}$	1.10	<i>PLEK</i>	Intergenic
rs9989735	2	231115454	C	0.18	$7.8 \times 10^{-14}$	1.17	0.19	$6.8 \times 10^{-11}$	1.14	$4.2 \times 10^{-23}$	1.16	<i>SP140</i>	Intronic
rs2371108	3	27757018	A	0.38	$2.1 \times 10^{-6}$	1.08	0.39	$5.8 \times 10^{-11}$	1.12	$1.5 \times 10^{-15}$	1.10	<i>EDMES</i>	downstream
rs1813375	3	28078571	A	0.47	$5.7 \times 10^{-18}$	1.15	0.49	$4.4 \times 10^{-16}$	1.15	$1.9 \times 10^{-32}$	1.15		Intergenic
rs1131265	3	119222456	C	0.80	$2.0 \times 10^{-15}$	1.19	0.81	$4.8 \times 10^{-10}$	1.14	$1.4 \times 10^{-23}$	1.17	<i>TIMMDC1</i>	Exonic
rs1920296 <sup>c</sup>	3	121543577	C	0.64	$6.8 \times 10^{-15}$	1.14	0.64	$5.5 \times 10^{-9}$	1.10	$6.5 \times 10^{-22}$	1.12	<i>IQCB1</i>	Intronic
rs2255214 <sup>c</sup>	3	121770539	C	0.52	$5.3 \times 10^{-13}$	1.13	0.52	$3.3 \times 10^{-13}$	1.13	$1.2 \times 10^{-24}$	1.13	<i>CD86</i>	Intergenic
rs1014486	3	159691112	G	0.43	$1.2 \times 10^{-9}$	1.11	0.44	$1.4 \times 10^{-10}$	1.11	$1.1 \times 10^{-18}$	1.11	<i>IL12A</i>	Intergenic
rs7665090	4	103551603	G	0.52	$2.4 \times 10^{-6}$	1.08	0.53	$5.0 \times 10^{-4}$	1.13	$1.0 \times 10^{-8}$	1.09	<i>MANBA</i>	Intergenic
rs6881706	5	35879156	C	0.72	$4.9 \times 10^{-9}$	1.12	0.73	$1.7 \times 10^{-9}$	1.12	$4.3 \times 10^{-17}$	1.12	<i>IL7R</i>	Intergenic
rs6880778	5	40399096	G	0.60	$1.7 \times 10^{-8}$	1.10	0.61	$3.9 \times 10^{-13}$	1.13	$8.1 \times 10^{-20}$	1.12		Intergenic
rs71624119	5	55440730	G	0.76	$2.7 \times 10^{-9}$	1.12	0.76	$1.9 \times 10^{-5}$	1.09	$3.4 \times 10^{-13}$	1.11	<i>ANKRD55</i>	Intronic
rs72928038	6	90976768	A	0.17	$7.6 \times 10^{-7}$	1.11	0.19	$9.0 \times 10^{-11}$	1.17	$1.5 \times 10^{-15}$	1.14	<i>BACH2</i>	Intronic
rs11154801	6	135739355	A	0.37	$2.3 \times 10^{-9}$	1.11	0.37	$1.0 \times 10^{-12}$	1.13	$1.8 \times 10^{-20}$	1.12	<i>AHI1</i>	Intronic
rs17066096	6	137452908	G	0.23	$5.9 \times 10^{-12}$	1.14	0.25	$4.1 \times 10^{-13}$	1.15	$1.6 \times 10^{-23}$	1.14	<i>IL22RA2</i>	Intergenic
rs67297943	6	138244816	A	0.78	$4.8 \times 10^{-8}$	1.12	0.80	$2.5 \times 10^{-6}$	1.11	$5.5 \times 10^{-13}$	1.11	<i>TNFAIP3</i>	Intergenic
rs212405	6	159470559	T	0.62	$1.4 \times 10^{-15}$	1.15	0.64	$1.8 \times 10^{-7}$	1.10	$8.0 \times 10^{-21}$	1.12	<i>TAGAP</i>	Intergenic
rs1021156	8	79575804	A	0.24	$5.6 \times 10^{-10}$	1.12	0.26	$2.1 \times 10^{-8}$	1.11	$8.5 \times 10^{-17}$	1.11	<i>ZC2HC1A</i>	Intergenic
rs4410871	8	128815029	G	0.72	$2.0 \times 10^{-9}$	1.12	0.72	$3.4 \times 10^{-8}$	1.11	$4.3 \times 10^{-16}$	1.11	<i>MIR1204</i>	Intergenic
rs759648	8	129158945	C	0.31	$2.8 \times 10^{-6}$	1.09	0.31	$3.7 \times 10^{-5}$	1.08	$5.0 \times 10^{-10}$	1.08	<i>MIR1208</i>	Intergenic
rs2104286	10	6099045	A	0.72	$7.6 \times 10^{-23}$	1.21	0.73	$3.6 \times 10^{-26}$	1.23	$2.3 \times 10^{-47}$	1.22	<i>IL2RA</i>	Intronic
rs1782645	10	81048611	A	0.43	$4.3 \times 10^{-7}$	1.09	0.41	$6.2 \times 10^{-10}$	1.11	$2.5 \times 10^{-15}$	1.10	<i>ZMIZ1</i>	Intronic
rs7923837	10	94481917	G	0.61	$4.6 \times 10^{-9}$	1.11	0.62	$2.0 \times 10^{-9}$	1.11	$4.3 \times 10^{-17}$	1.11	<i>HHEX</i>	Intergenic
rs34383631	11	60793330	A	0.40	$5.7 \times 10^{-10}$	1.11	0.39	$4.5 \times 10^{-15}$	1.15	$3.7 \times 10^{-23}$	1.13	<i>CD6</i>	Intergenic
rs1800693	12	6440009	G	0.40	$6.9 \times 10^{-16}$	1.14	0.41	$1.0 \times 10^{-13}$	1.14	$6.7 \times 10^{-28}$	1.14	<i>TNFRSF1A</i>	Intronic
rs11052877	12	9905690	G	0.36	$5.4 \times 10^{-9}$	1.10	0.38	$1.2 \times 10^{-5}$	1.08	$5.6 \times 10^{-13}$	1.09	<i>CD69</i>	3' UTR
rs201202118 <sup>d</sup>	12	58182062	A	0.67	$7.4 \times 10^{-13}$	1.14	0.67	$1.6 \times 10^{-10}$	1.12	$9.0 \times 10^{-22}$	1.13	<i>TSFM</i>	Intronic
rs7132277	12	123593382	A	0.19	$1.9 \times 10^{-6}$	1.10	0.19	$1.4 \times 10^{-8}$	1.13	$1.9 \times 10^{-13}$	1.12	<i>PITPNM2</i>	Intronic
rs2236262	14	69261472	A	0.50	$1.2 \times 10^{-5}$	1.08	0.50	$3.8 \times 10^{-8}$	1.09	$2.5 \times 10^{-12}$	1.08	<i>ZFP36L1</i>	Intronic
rs74796499	14	88432328	C	0.95	$8.5 \times 10^{-11}$	1.31	0.95	$4.5 \times 10^{-11}$	1.33	$2.4 \times 10^{-20}$	1.32	<i>GALC</i>	Intronic
rs12927355	16	11194771	G	0.68	$8.2 \times 10^{-27}$	1.21	0.69	$4.3 \times 10^{-21}$	1.18	$6.4 \times 10^{-46}$	1.20	<i>CLEC16A</i>	Intronic
rs35929052	16	85994484	G	0.89	$3.3 \times 10^{-7}$	1.14	0.88	$3.6 \times 10^{-6}$	1.15	$5.9 \times 10^{-12}$	1.15	<i>IRF8</i>	Intergenic
rs4796791	17	40530763	A	0.36	$1.8 \times 10^{-8}$	1.10	0.36	$1.2 \times 10^{-13}$	1.14	$3.7 \times 10^{-20}$	1.12	<i>STAT3</i>	Intronic
rs8070345	17	57816757	A	0.45	$5.4 \times 10^{-16}$	1.14	0.46	$1.9 \times 10^{-9}$	1.10	$2.2 \times 10^{-23}$	1.12	<i>VMP1</i>	Intronic
rs1077667	19	6668972	G	0.79	$3.5 \times 10^{-13}$	1.16	0.79	$8.4 \times 10^{-13}$	1.16	$1.7 \times 10^{-24}$	1.16	<i>TNFSF14</i>	Intronic
rs34536443	19	10463118	C	0.95	$1.2 \times 10^{-8}$	1.28	0.96	$2.9 \times 10^{-7}$	1.30	$1.8 \times 10^{-14}$	1.29	<i>TYK2</i>	Exonic
rs11554159	19	18285944	G	0.73	$2.6 \times 10^{-13}$	1.15	0.74	$1.4 \times 10^{-12}$	1.15	$1.9 \times 10^{-24}$	1.15	<i>IFI30</i>	Exonic
rs8107548	19	49870643	G	0.25	$2.0 \times 10^{-6}$	1.09	0.26	$2.5 \times 10^{-10}$	1.13	$5.7 \times 10^{-15}$	1.11	<i>DKKL1</i>	Intronic
rs4810485	20	44747947	A	0.25	$1.8 \times 10^{-5}$	1.08	0.25	$1.4 \times 10^{-12}$	1.14	$7.7 \times 10^{-16}$	1.11	<i>CD40</i>	Intronic
rs2248359	20	52791518	G	0.60	$9.8 \times 10^{-5}$	1.07	0.62	$8.2 \times 10^{-11}$	1.12	$2.0 \times 10^{-13}$	1.09	<i>CYP24A1</i>	Intergenic
rs2283792	22	22131125	C	0.51	$1.1 \times 10^{-6}$	1.08	0.53	$5.4 \times 10^{-11}$	1.11	$5.5 \times 10^{-16}$	1.10	<i>MAPK1</i>	Intronic
<b>Secondary</b>													
rs523604 <sup>e</sup>	11	118755738	A	0.53	$2.5 \times 10^{-7}$	1.09	0.54	$4.0 \times 10^{-9}$	1.11	$6.2 \times 10^{-15}$	1.10	<i>CXCR5</i>	Intronic

All listed signals had discovery  $P \leq 1.0 \times 10^{-4}$ , replication  $P \leq 5.0 \times 10^{-2}$  and joint  $P \leq 5.0 \times 10^{-8}$ . All *P* values are two-sided. Chr., chromosome; RA, risk allele; RAF, risk allele frequency.

<sup>a</sup>Position is based on hg19 and dbSNP Build 137. <sup>b</sup>The nearest gene is listed if it lies within 50 kb of the signal. Bold font indicates genes that are part of GO immune system process. <sup>c</sup>These three SNPs were not primary in the 2011 GWAS<sup>9</sup> (two were secondary, and the third was tertiary in that study). <sup>d</sup>A proxy SNP (rs10431552;  $r^2 = 0.99$ ) was used in replication. <sup>e</sup>The *P* values and OR values shown are after conditioning on rs9736016 and rs533646 (Table 1).

More specifically, ~9.1% overlapped signals in inflammatory bowel disease, ~7.3% overlapped signals in ulcerative colitis, ~9.1% overlapped signals in Crohn's disease<sup>15</sup>, ~9.1% overlapped signals in primary biliary cirrhosis<sup>32,33</sup>, ~4.5% overlapped signals in celiac disease<sup>34</sup>, ~4.5% overlapped signals in rheumatoid arthritis<sup>35</sup>, ~0.9% overlapped signals in psoriasis<sup>36</sup>, and ~2.7% overlapped signals in autoimmune thyroid disease<sup>37</sup>. We report at seven loci the same top variant seen in primary biliary cirrhosis. We also note that our best

*TYK2* variant (rs34536443)<sup>38</sup> is also the most associated *TYK2* variant for primary biliary cirrhosis, psoriasis and rheumatoid arthritis. Lastly, variants have been reported for autoimmune thyroid disease, celiac disease, primary biliary cirrhosis and rheumatoid arthritis that have pairwise  $r^2 \geq 0.8$  with the multiple sclerosis risk variant near *MMEL1* (Supplementary Table 8)<sup>39</sup>.

In summary, we have identified 48 new susceptibility variants for multiple sclerosis. These newly discovered loci expand our understanding

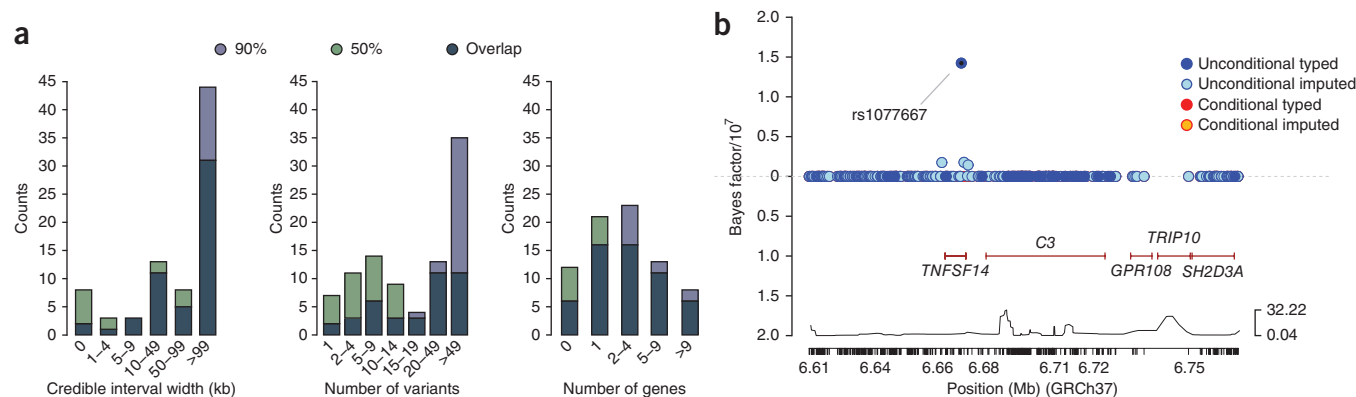


**Figure 2** Bayesian fine mapping within primary regions of association. (a) Summary of the extent of fine mapping across 66 regions in 6,356 subjects with multiple sclerosis and 9,617 healthy controls from the UK, showing the physical extent of the number of variants and the number of genes spanned by the posterior 90% and 50% credible sets. (b) Details of fine mapping in the region encompassing *TNFSF14*. Bayes factors summarizing evidence for association of the SNPs before conditioning on the lead SNP (rs1077667) are shown above the x axis (blue markers), and the Bayes factors after conditioning are shown below the x axis.

**Table 3 Results for 18 variants from the 8 regions with consistent high-resolution fine mapping**

Gene	SNP	Chr.	Position <sup>a</sup>	Posterior	GERP	Functional annotation <sup>b</sup>
<i>IL2RA</i>	rs2104286	10	6099045	0.93	-0.47	Intronic, correlates with soluble IL-2RA levels
<i>TNFSF14</i>	rs1077667	19	6668972	0.74	-3.89	Intronic, TFBS or DNase I peak, correlates with serum levels of <i>TNFSF14</i>
<i>TNFRSF1A</i>	rs1800693	12	6440009	0.69	2.53	Intronic, causes splicing defect and truncated soluble <i>TNFRSF1A</i>
	rs4149580 <sup>c</sup>	12	6446990	0.10	2.06	intronic
<i>IL12A</i>	rs1014486	3	159691112	0.67	0.24	-
<i>STAT4</i>	rs78712823	2	191958581	0.59	-3.98	Intronic
<i>TNFAIP3</i>	rs632574	6	137959118	0.27	-1.15	-
	rs498549 <sup>c</sup>	6	137984935	0.20	0.52	-
	rs651973	6	137996134	0.17	2.41	Downstream of RP11-95M15.1 lincRNA gene
	rs536331	6	137993049	0.15	0.19	Upstream of RP11-95M15.1 lincRNA gene
<i>CD58</i>	rs35275493 <sup>c</sup>	1	117095502	0.24	0.75	Intronic (insertion)
	rs10754324 <sup>c</sup>	1	117093035	0.22	0.32	Intronic
	rs6677309	1	117080166	0.21	-1.18	Intronic, TFBS or DNase I peak
	rs1335532	1	117100957	0.17	-1.32	Intronic
<i>CD6</i>	rs34383631	11	60793330	0.20	1.66	-
	rs4939490 <sup>c</sup>	11	60793651	0.14	-0.53	-
	rs4939491 <sup>c</sup>	11	60793722	0.14	-0.37	-
	rs4939489	11	60793648	0.10	3.25	-

All listed variants have posterior probability  $\geq 0.1$  in regions where  $\leq 5$  variants explain the top 50% of the posterior probability, and the top SNP from the frequentist analysis resides in the 90% confidence interval; SNPs are ordered by maximum posterior probability within each region. Posterior probability is the probability of any variant driving association<sup>23</sup>. GERP denotes Genomic Evolutionary Rate Profiling. Chr., chromosome; TFBS, transcription factor binding site; lincRNA, long noncoding RNA.

<sup>a</sup>Position is based on hg19 and dbSNP Build 137. <sup>b</sup>Functional data are from VEP, the eQTL browser, Fairfax *et al.*<sup>20</sup>, PubMed searches and the 1000 Genomes Project. Minus signs indicate intergenic signals with no additional annotation and no reported regulatory consequence. <sup>c</sup>Imputed variant.

of the immune system processes implicated in multiple sclerosis. We estimate that the 110 established non-MHC risk variants explain 20% of the sibling recurrence risk, 28% when including the already identified MHC effects<sup>9</sup> (**Supplementary Note**). Additionally, we have identified five previously associated regions (*TNFSF14*, *IL2RA*, *TNFRSF1A*, *IL12A* and *STAT4*) where consistent high-resolution fine mapping implicated one variant that accounted for more than 50% of the posterior probability of association. Our study further implicates NF- $\kappa$ B in multiple sclerosis pathobiology<sup>18</sup>, emphasizes the value of dense fine mapping in large follow-up data sets and exposes the urgent need for functional annotation in relevant tissues. Understanding the implicated networks and their relationship to environmental risk factors will promote the development of rational therapies and may enable the development of preventive strategies.

**URLs.** ImmunoBase, <http://www.immunobase.org/>; eQTL browser, <http://eqtl.uchicago.edu/>; MetaCore, <https://portal.genego.com/>.

## METHODS

Methods and any associated references are available in the [online version of the paper](#).

*Note: Any Supplementary Information and Source Data files are available in the online version of the paper.*

## ACKNOWLEDGMENTS

We thank the participants, the referring nurses, the physicians and the funders. Funding was provided by the US National Institutes of Health, the Wellcome Trust, the UK MS Society, the UK Medical Research Council, the US National MS Society, the Cambridge National Institute for Health Research (NIHR) Biomedical Research Centre, DeNDRon, the Bibbi and Niels Jensens Foundation, the Swedish Brain Foundation, the Swedish Research Council, the Knut and Alice Wallenberg Foundation, the Swedish Heart-Lung Foundation, the Foundation for Strategic Research, the Stockholm County Council, Karolinska Institutet, INSERM, Fondation d'Aide pour la Recherche sur la Sclérose en Plaques, Association Française contre les Myopathies, Infrastructures en Biologie Santé et Agronomie (GIS-IBISA), the German Ministry for Education and Research, the German Competence Network MS, Deutsche Forschungsgemeinschaft,

Munich Biotech Cluster M4, the Fidelity Biosciences Research Initiative, Research Foundation Flanders, Research Fund KU Leuven, the Belgian Charcot Foundation, Gemeinnützige Hertie Stiftung, University Zurich, the Danish MS Society, the Danish Council for Strategic Research, the Academy of Finland, the Sigrid Juselius Foundation, Helsinki University, the Italian MS Foundation, Fondazione Cariplo, the Italian Ministry of University and Research, the Torino Savings Bank Foundation, the Italian Ministry of Health, the Italian Institute of Experimental Neurology, the MS Association of Oslo, the Norwegian Research Council, the South-Eastern Norwegian Health Authorities, the Australian National Health and Medical Research Council, the Dutch MS Foundation and Kaiser Permanente. We acknowledge the British 1958 Birth Cohort, the UK National Blood Service, Vanderbilt University Medical Center's BioVU DNA Research Core, Centre de Ressources Biologiques du Réseau Français d'Etude Génétique de la Sclérose en Plaques, the Norwegian Bone Marrow Registry, the Norwegian MS Registry and Biobank, the North American Research Committee on MS Registry, the Brigham and Women's Hospital PhenoGenetic Project and DILGOM, funded by the Academy of Finland. See the **Supplementary Note** for details.

#### AUTHOR CONTRIBUTIONS

M.F.D., D. Booth, A.O., J.S., B. Fontaine, B.H., C. Martin, F.Z., S.D., F.M.-B., B.T., H.F.H., I. Kockum, J. Hillert, T.O., J.R.O., R.H., L.F.B., C. Agliardi, L.A., L. Bernardinelli, V.B., S.B., B.B., L. Brundin, D. Buck, H. Butzkueven, W. Camu, P.C., E.G.C., I.C., G.C., I.C.-R., B.A.C.C., G.D., S.R.D., A.d.S., B.D., M.D., I.E., F.E., N.E., J.F., A.F., I.Y.F., D.G., C. Graetz, A. Graham, C. Guaschino, C. Halfpenny, G. Hall, J. Harley, T.H., C. Hawkins, C. Hillier, J. Hobart, M.H., I.J., A.J., B.K., A. Kermode, T. Kilpatrick, K.K., T. Korn, H.K., C.L.-F., J.L.-S., M.H.L., M.A.L., G.L., B.A.L., C.M.L., F.L., J. Lycke, S.M., C.P.M., R.M., V.M., D.M., G. Mazibrada, J.M., K.-M.M., G.N., R.N., P.N., F.P., S.E.P., H.Q., M. Reunanen, W.R., N.P.R., M. Rodegher, D.R., M. Salvetti, F.S., R.C.S., C. Schaefer, S. Shaunak, L.S., S. Shields, V.S., M. Slee, P.S.S., M. Sospedra, A. Spurkland, V.T., J.T., A.T., P.T., C.v.D., E.M.V., S.V., J.S.W., A.W., J.F.W., J.Z., E.Z., J.L.H., M.A.P.-V., G.S., D.H., S.L.H., A.C., P.D.J., S.J.S. and J.L.M. were involved with case ascertainment and phenotyping. A. Kempainen, D. Booth, A. Goris, A.O., B. Fontaine, S.D., F.M.-B., H.F.H., I. Kockum, M.B., J.R.O., L.F.B., IIBDGC, H.B.S., A. Baker, N.B., L. Bergamaschi, I.L.B., P.B., D. Buck, S.J.C., L. Corrado, L. Cosemans, I.C.-R., V.D., J.F., A.F., V.G., I.J., I. Konidari, V.L., C.M.L., M. Lindén, J. Link, C. McCabe, I.-L.M., H.Q., M. Sorosina, E.S., H.W., P.D.J., S.J.S. and J.L.M. processed the DNA. A. Kempainen, A.O., B. Fontaine, M.B., R.H., L.F.B., WTCCC2, IIBDGC, R.A., H.B.S., N.B., T.M.C.B., H. Blackburn, P.B., W. Carpentier, L. Corrado, I.C.-R., D.C., V.D., P. Deloukas, S.E., A.F., H.H., P.H., A. Hamsten, S.E.H., I.J., I. Konidari, C.L., M. Larsson, M. Lathrop, F.M., I.-L.M., J.M., H.Q., F.S., M. Sorosina, C.V.D., J.W., D.H., P.D.J., S.J.S. and J.L.M. conducted and supervised the genotyping of samples. A.H.B., N.A.P., D.K.X., M.F.D., A. Kempainen, C.C., T.S.S., C. Spencer, M.B., IIBDGC, C. Anderson, S.E.B., A.T.D., P. Donnelly, B. Fiddes, P.-A.G., G. Hellenthal, S.E.H., L.M., M.P., N.C.S.-B., J.L.H., M.A.P.-V., G. McVean, P.D.J., S.J.S. and J.L.M. performed the statistical analysis. A.H.B., N.A.P., D.K.X., M.F.D., A. Kempainen, C.C., T.S.S., C. Spencer, D. Booth, A. Goris, A.O., J.S., B. Fontaine, B.H., F.Z., S.D., F.M.-B., H.F.H., I. Kockum, M.B., R.H., L.F.B., C. Agliardi, M.A., C. Anderson, R.A., H.B.S., A. Baker, G.B., N.B., J.B., C.B., L. Bernardinelli, A. Berthele, V.B., T.M.C.B., H. Blackburn, I.L.B., B.B., D. Buck, S.J.C., W. Camu, P.C., E.G.C., I.C., G.C., L. Corrado, L. Cosemans, I.C.-R., B.A.C.C., D.C., G.D., S.R.D., P. Deloukas, A.d.S., A.T.D., P. Donnelly, B.D., M.D., S.E., F.E., N.E., B. Fiddes, J.F., A.F., C.F., D.G., C. Gieger, C. Graetz, A. Graham, V.G., C. Guaschino, A. Hadjixenofontos, H.H., C. Halfpenny, P.H., G. Hall, A. Hamsten, J. Harley, T.H., C. Hawkins, G. Hellenthal, C. Hillier, J. Hobart, M.H., S.E.H., I.J., A.J., B.K., I. Konidari, H.K., C.L., M. Larsson, M. Lathrop, C.L.-F., M.A.L., V.L., G.L., B.A.L., C.M.L., F.M., C.P.M., R.M., V.M., G. Mazibrada, C. McCabe, I.-L.M., L.M., K.-M.M., R.N., M.P., S.E.P., H.Q., N.P.R., M. Rodegher, D.R., M. Salvetti, N.C.S.-B., R.C.S., C. Schaefer, S. Shaunak, L.S., S. Shields, M. Sospedra, A. Strange, J.T., A.T., E.M.V., A.W., J.F.W., J.W., J.Z., J.L.H., A.J.I., G. McVean, P.D.J., S.J.S. and J.L.M. collected and managed the project data. A.H.B., N.A.P., M.F.D., A. Kempainen, C.C., T.S.S., C. Spencer, J.S., B.H., F.Z., S.D., F.M.-B., H.F.H., J. Hillert, T.O., M.B., J.R.O., R.H., L.F.B., L.A., C. Anderson, G.B., J.B., C.B., A. Berthele, E.G.C., G.C., P. Donnelly, F.E., C.F., C. Gieger, C. Graetz, G. Hellenthal, M.J., T. Korn, M.A.L., R.M., M.P., M. Sospedra, A. Spurkland, A. Strange, J.W., J.L.H., M.A.P.-V., A.J.I., G.S., D.H., S.L.H., A.C., G. McVean, P.D.J., S.J.S. and J.L.M. contributed to the study concept and design. A.H.B., N.A.P., D.K.X., G. McVean, P.D.J., S.J.S. and J.L.M. prepared the manuscript. All authors reviewed the final manuscript.

#### COMPETING FINANCIAL INTERESTS

The authors declare no competing financial interests.

Reprints and permissions information is available online at <http://www.nature.com/reprints/index.html>.

- Gourraud, P.A., Harbo, H.F., Hauser, S.L. & Baranzini, S.E. The genetics of multiple sclerosis: an up-to-date review. *Immunol. Rev.* **248**, 87–103 (2012).
- Nylander, A. & Hafler, D.A. Multiple sclerosis. *J. Clin. Invest.* **122**, 1180–1188 (2012).
- Compston, A. *et al.* *McAlpine's Multiple Sclerosis* (Churchill Livingstone, London, 2006).
- Dyment, D.A., Yee, I.M., Ebers, G.C. & Sadovnick, A.D. Multiple sclerosis in stepsiblings: recurrence risk and ascertainment. *J. Neurol. Neurosurg. Psychiatry* **77**, 258–259 (2006).
- Hemminki, K., Li, X., Sundquist, J., Hillert, J. & Sundquist, K. Risk for multiple sclerosis in relatives and spouses of patients diagnosed with autoimmune and related conditions. *Neurogenetics* **10**, 5–11 (2009).
- Jersild, C., Svejgaard, A. & Fog, T. HL-A antigens and multiple sclerosis. *Lancet* **1**, 1240–1241 (1972).
- International Multiple Sclerosis Genetics Consortium. Risk alleles for multiple sclerosis identified by a genome-wide study. *N. Engl. J. Med.* **357**, 851–862 (2007).
- De Jager, P.L. *et al.* Meta-analysis of genome scans and replication identify *CD6*, *IRF8* and *TNFRSF1A* as new multiple sclerosis susceptibility loci. *Nat. Genet.* **41**, 776–782 (2009).
- International Multiple Sclerosis Genetics Consortium & Wellcome Trust Case Control Consortium 2. Genetic risk and a primary role for cell-mediated immune mechanisms in multiple sclerosis. *Nature* **476**, 214–219 (2011).
- Patsopoulos, N.A. *et al.* Genome-wide meta-analysis identifies novel multiple sclerosis susceptibility loci. *Ann. Neurol.* **70**, 897–912 (2011).
- International Multiple Sclerosis Genetics Consortium. Evidence for polygenic susceptibility to multiple sclerosis—the shape of things to come. *Am. J. Hum. Genet.* **86**, 621–625 (2010).
- Baranzini, S.E. The genetics of autoimmune diseases: a networked perspective. *Curr. Opin. Immunol.* **21**, 596–605 (2009).
- Cotsapas, C. *et al.* Pervasive sharing of genetic effects in autoimmune disease. *PLoS Genet.* **7**, e1002254 (2011).
- Cortes, A. & Brown, M.A. Promise and pitfalls of the Immunochip. *Arthritis Res. Ther.* **13**, 101 (2011).
- Jostins, L. *et al.* Host-microbe interactions have shaped the genetic architecture of inflammatory bowel disease. *Nature* **491**, 119–124 (2012).
- Krzyszowski, M. *et al.* Circo: an information aesthetic for comparative genomics. *Genome Res.* **19**, 1639–1645 (2009).
- Willis, T.G. *et al.* *Bcl10* is involved in t(1;14)(p22;q32) of MALT B cell lymphoma and mutated in multiple tumor types. *Cell* **96**, 35–45 (1999).
- Yan, J. & Greer, J.M. NF- $\kappa$ B, a potential therapeutic target for the treatment of multiple sclerosis. *CNS Neurol. Disord. Drug Targets* **7**, 536–557 (2008).
- Wegener, E. & Krappmann, D. CARD-Bcl10-Malt1 signalosomes: missing link to NF- $\kappa$ B. *Sci. STKE* **2007**, pe21 (2007).
- Fairfax, B.P. *et al.* Genetics of gene expression in primary immune cells identifies cell type-specific master regulators and roles of HLA alleles. *Nat. Genet.* **44**, 502–510 (2012).
- Lill, C.M. *et al.* Genome-wide significant association of *ANKRD55* rs6859219 and multiple sclerosis risk. *J. Med. Genet.* **50**, 140–143 (2013).
- Maier, L.M. *et al.* *IL2RA* genetic heterogeneity in multiple sclerosis and type 1 diabetes susceptibility and soluble interleukin-2 receptor production. *PLoS Genet.* **5**, e1000322 (2009).
- Maller, J.B. *et al.* Bayesian refinement of association signals for 14 loci in 3 common diseases. *Nat. Genet.* **44**, 1294–1301 (2012).
- McLaren, W. *et al.* Deriving the consequences of genomic variants with the Ensembl API and SNP Effect Predictor. *Bioinformatics* **26**, 2069–2070 (2010).
- Gregory, A.P. *et al.* TNF receptor 1 genetic risk mirrors outcome of anti-TNF therapy in multiple sclerosis. *Nature* **488**, 508–511 (2012).
- De Jager, P.L. *et al.* The role of the *CD58* locus in multiple sclerosis. *Proc. Natl. Acad. Sci. USA* **106**, 5264–5269 (2009).
- Malmström, C. *et al.* Serum levels of LIGHT in MS. *Mult. Scler.* **19**, 871–876 (2013).
- ENCODE Project Consortium. An integrated encyclopedia of DNA elements in the human genome. *Nature* **489**, 57–74 (2012).
- Schaub, M.A., Boyle, A.P., Kundaje, A., Batzoglou, S. & Snyder, M. Linking disease associations with regulatory information in the human genome. *Genome Res.* **22**, 1748–1759 (2012).
- Davydov, E.V. *et al.* Identifying a high fraction of the human genome to be under selective constraint using GERP++. *PLoS Comput. Biol.* **6**, e1001025 (2010).
- Johnson, A.D. *et al.* SNAP: a web-based tool for identification and annotation of proxy SNPs using HapMap. *Bioinformatics* **24**, 2938–2939 (2008).
- Juran, B.D. *et al.* Immunochip analyses identify a novel risk locus for primary biliary cirrhosis at 13q14, multiple independent associations at four established risk loci and epistasis between 1p31 and 7q32 risk variants. *Hum. Mol. Genet.* **21**, 5209–5221 (2012).
- Liu, J.Z. *et al.* Dense fine-mapping study identifies new susceptibility loci for primary biliary cirrhosis. *Nat. Genet.* **44**, 1137–1141 (2012).
- Trynka, G. *et al.* Dense genotyping identifies and localizes multiple common and rare variant association signals in celiac disease. *Nat. Genet.* **43**, 1193–1201 (2011).
- Eyre, S. *et al.* High-density genetic mapping identifies new susceptibility loci for rheumatoid arthritis. *Nat. Genet.* **44**, 1336–1340 (2012).
- Tsoi, L.C. *et al.* Identification of 15 new psoriasis susceptibility loci highlights the role of innate immunity. *Nat. Genet.* **44**, 1341–1348 (2012).
- Cooper, J.D. *et al.* Seven newly identified loci for autoimmune thyroid disease. *Hum. Mol. Genet.* **21**, 5202–5208 (2012).
- Ban, M. *et al.* Replication analysis identifies *TYK2* as a multiple sclerosis susceptibility factor. *Eur. J. Hum. Genet.* **17**, 1309–1313 (2009).
- Ban, M. *et al.* A non-synonymous SNP within membrane metalloendopeptidase-like 1 (*MMEL1*) is associated with multiple sclerosis. *Genes Immun.* **11**, 660–664 (2010).

Ashley H Beecham<sup>1,127</sup>, Nikolaos A Patsopoulos<sup>2-6,127</sup>, Dionysia K Xifara<sup>7</sup>, Mary F Davis<sup>8</sup>, Anu Kempainen<sup>9</sup>, Chris Cotsapas<sup>10-12</sup>, Tejas S Shah<sup>13</sup>, Chris Spencer<sup>7</sup>, David Booth<sup>14</sup>, An Goris<sup>15</sup>, Annette Oturai<sup>16</sup>, Janna Saarela<sup>17</sup>, Bertrand Fontaine<sup>18</sup>, Bernhard Hemmer<sup>19-21</sup>, Claes Martin<sup>22</sup>, Frauke Zipp<sup>23</sup>, Sandra D'Alfonso<sup>24,25</sup>, Filippo Martinelli-Boneschi<sup>26,27</sup>, Bruce Taylor<sup>28</sup>, Hanne F Harbo<sup>29,30</sup>, Ingrid Kockum<sup>31</sup>, Jan Hillert<sup>31</sup>, Tomas Olsson<sup>31</sup>, Maria Ban<sup>9</sup>, Jorge R Oksenberg<sup>32</sup>, Rogier Hintzen<sup>33</sup>, Lisa F Barcellos<sup>34-36</sup>, Wellcome Trust Case Control Consortium 2 (WTCCC2)<sup>37</sup>, International IBD Genetics Consortium (IIBDGC)<sup>37</sup>, Cristina Agliardi<sup>38</sup>, Lars Alfredsson<sup>39</sup>, Mehdi Alizadeh<sup>40</sup>, Carl Anderson<sup>13</sup>, Robert Andrews<sup>13</sup>, Helle Bach Søndergaard<sup>16</sup>, Amie Baker<sup>9</sup>, Gavin Band<sup>7</sup>, Sergio E Baranzini<sup>32</sup>, Nadia Barizzone<sup>24,25</sup>, Jeffrey Barrett<sup>13</sup>, Céline Bellenguez<sup>7</sup>, Laura Bergamaschi<sup>24,25</sup>, Luisa Bernardinelli<sup>41</sup>, Achim Berthele<sup>19</sup>, Viola Biberacher<sup>19</sup>, Thomas M C Binder<sup>42</sup>, Hannah Blackburn<sup>13</sup>, Izaaura L Bomfim<sup>31</sup>, Paola Brambilla<sup>26</sup>, Simon Broadley<sup>43</sup>, Bruno Brochet<sup>44</sup>, Lou Brundin<sup>31</sup>, Dorothea Buck<sup>19</sup>, Helmut Butzkueven<sup>45,46</sup>, Stacy J Caillier<sup>32</sup>, William Camu<sup>47</sup>, Wassila Carpentier<sup>48</sup>, Paola Cavalla<sup>49,50</sup>, Elisabeth G Celius<sup>29</sup>, Irène Coman<sup>51</sup>, Giancarlo Comi<sup>26,27</sup>, Lucia Corrado<sup>24,25</sup>, Leentje Cosemans<sup>15</sup>, Isabelle Cournu-Rebeix<sup>18</sup>, Bruce A C Cree<sup>32</sup>, Daniele Cusi<sup>52</sup>, Vincent Damotte<sup>18</sup>, Gilles Defer<sup>53</sup>, Silvia R Delgado<sup>54</sup>, Panos Deloukas<sup>13</sup>, Alessia di Sapio<sup>55</sup>, Alexander T Dilthey<sup>7</sup>, Peter Donnelly<sup>7</sup>, Bénédicte Dubois<sup>15</sup>, Martin Duddy<sup>56</sup>, Sarah Edkins<sup>13</sup>, Irina Elovaara<sup>57</sup>, Federica Esposito<sup>26,27</sup>, Nikos Evangelou<sup>58</sup>, Barnaby Fiddes<sup>9</sup>, Judith Field<sup>59</sup>, Andre Franke<sup>60</sup>, Colin Freeman<sup>7</sup>, Irene Y Frohlich<sup>2</sup>, Daniela Galimberti<sup>61,62</sup>, Christian Gieger<sup>63</sup>, Pierre-Antoine Gourraud<sup>32</sup>, Christiane Graetz<sup>23</sup>, Andrew Graham<sup>64</sup>, Verena Grummel<sup>19</sup>, Clara Guaschino<sup>26,27</sup>, Athena Hadjixenofontos<sup>1</sup>, Hakon Hakonarson<sup>65,66</sup>, Christopher Halfpenny<sup>67</sup>, Gillian Hall<sup>68</sup>, Per Hall<sup>69</sup>, Anders Hamsten<sup>70</sup>, James Harley<sup>71</sup>, Timothy Harrower<sup>72</sup>, Clive Hawkins<sup>73</sup>, Garrett Hellenthal<sup>74</sup>, Charles Hillier<sup>75</sup>, Jeremy Hobart<sup>76</sup>, Muni Hoshi<sup>19</sup>, Sarah E Hunt<sup>13</sup>, Maja Jagodic<sup>31</sup>, Ilijas Jelčić<sup>77,78</sup>, Angela Jochim<sup>19</sup>, Brian Kendall<sup>79</sup>, Allan Kermodé<sup>80,81</sup>, Trevor Kilpatrick<sup>82</sup>, Keijo Koivisto<sup>83</sup>, Ioanna Konidari<sup>1</sup>, Thomas Korn<sup>19</sup>, Helena Kronsbein<sup>19</sup>, Cordelia Langford<sup>13</sup>, Malin Larsson<sup>84</sup>, Mark Lathrop<sup>85-87</sup>, Christine Lebrun-Frenay<sup>88</sup>, Jeannette Lechner-Scott<sup>89</sup>, Michelle H Lee<sup>2</sup>, Maurizio A Leone<sup>90</sup>, Virpi Leppä<sup>17</sup>, Giuseppe Liberatore<sup>26,27</sup>, Benedicte A Lie<sup>30,91</sup>, Christina M Lill<sup>23,92</sup>, Magdalena Lindén<sup>31</sup>, Jenny Link<sup>31</sup>, Felix Luessi<sup>23</sup>, Jan Lycke<sup>93</sup>, Fabio Macchiardi<sup>94,95</sup>, Satu Männistö<sup>96</sup>, Clara P Manrique<sup>1</sup>, Roland Martin<sup>77,78</sup>, Vittorio Martinelli<sup>27</sup>, Deborah Mason<sup>97</sup>, Gordon Mazibrada<sup>98</sup>, Cristin McCabe<sup>10</sup>, Inger-Lise Mero<sup>29,30,91</sup>, Julia Mescheriakova<sup>33</sup>, Loukas Moutsianas<sup>7</sup>, Kjell-Morten Myhr<sup>99</sup>, Guy Nagels<sup>100</sup>, Richard Nicholas<sup>101</sup>, Petra Nilsson<sup>102</sup>, Fredrik Piehl<sup>31</sup>, Matti Pirinen<sup>7</sup>, Siân E Price<sup>103</sup>, Hong Quach<sup>34</sup>, Mauri Reunanen<sup>104,105</sup>, Wim Robberecht<sup>106-108</sup>, Neil P Robertson<sup>109</sup>, Mariaemma Rodegher<sup>27</sup>, David Rog<sup>110</sup>, Marco Salvetti<sup>111</sup>, Nathalie C Schnetz-Boutaud<sup>8</sup>, Finn Sellebjerg<sup>16</sup>, Rebecca C Selter<sup>19</sup>, Catherine Schaefer<sup>36</sup>, Sandip Shaunak<sup>112</sup>, Ling Shen<sup>36</sup>, Simon Shields<sup>113</sup>, Volker Siffrin<sup>23</sup>, Mark Slee<sup>114</sup>, Per Soelberg Sorensen<sup>16</sup>, Melissa Sorosina<sup>26</sup>, Mireia Sospedra<sup>77,78</sup>, Anne Spurkland<sup>115</sup>, Amy Strange<sup>7</sup>, Emilie Sundqvist<sup>31</sup>, Vincent Thijs<sup>106-108</sup>, John Thorpe<sup>116</sup>, Anna Ticca<sup>117</sup>, Pentti Tienari<sup>118</sup>, Cornelia van Duijn<sup>119</sup>, Elizabeth M Visser<sup>120</sup>, Steve Vucic<sup>14</sup>, Helga Westerlind<sup>31</sup>, James S Wiley<sup>59</sup>, Alastair Wilkins<sup>121</sup>, James F Wilson<sup>122</sup>, Juliane Winkelmann<sup>19,20,123,124</sup>, John Zajicek<sup>76</sup>, Eva Zindler<sup>23</sup>, Jonathan L Haines<sup>8</sup>, Margaret A Pericak-Vance<sup>1</sup>, Adrian J Ivinson<sup>125</sup>, Graeme Stewart<sup>14</sup>, David Hafler<sup>10,11,126</sup>, Stephen L Hauser<sup>32</sup>, Alastair Compston<sup>9</sup>, Gil McVean<sup>7</sup>, Philip De Jager<sup>2,5,10,127,128</sup>, Stephen J Sawcer<sup>9,127,128</sup> & Jacob L McCauley<sup>1,127,128</sup>

<sup>1</sup>John P. Hussman Institute for Human Genomics, University of Miami, Miller School of Medicine, Miami, Florida, USA. <sup>2</sup>Department of Neurology, Program in Translational NeuroPsychiatric Genomics, Institute for the Neurosciences, Brigham & Women's Hospital, Boston, Massachusetts, USA. <sup>3</sup>Department of Psychiatry, Program in Translational NeuroPsychiatric Genomics, Institute for the Neurosciences, Brigham & Women's Hospital, Boston, Massachusetts, USA. <sup>4</sup>Department of Medicine, Division of Genetics, Brigham & Women's Hospital, Harvard Medical School, Boston, Massachusetts, USA. <sup>5</sup>Harvard Medical School, Boston, Massachusetts, USA. <sup>6</sup>Broad Institute of Harvard and MIT, Cambridge, Massachusetts, USA. <sup>7</sup>The Wellcome Trust Centre for Human Genetics, University of Oxford, Oxford, UK. <sup>8</sup>Center for Human Genetics Research, Vanderbilt University Medical Center, Nashville, Tennessee, USA. <sup>9</sup>Department of Clinical Neurosciences, Addenbrooke's Hospital, University of Cambridge, Cambridge, UK. <sup>10</sup>Program in Medical and Population Genetics, Broad Institute of Harvard and MIT, Cambridge, Massachusetts, USA. <sup>11</sup>Department of Neurology, Yale University School of Medicine, New Haven, Connecticut, USA. <sup>12</sup>Department of Genetics, Yale University School of Medicine, New Haven, Connecticut, USA. <sup>13</sup>Wellcome Trust Sanger Institute, Wellcome Trust Genome Campus, Hinxton, Cambridge, UK. <sup>14</sup>Westmead Millennium Institute, University of Sydney, Westmead, New South Wales, Australia. <sup>15</sup>Section of Experimental Neurology, Laboratory for Neuroimmunology, KU Leuven, Leuven, Belgium. <sup>16</sup>Department of Neurology, Danish Multiple Sclerosis Center, Copenhagen University Hospital, Copenhagen, Denmark. <sup>17</sup>Institute for Molecular Medicine Finland, University of Helsinki, Helsinki, Finland. <sup>18</sup>Département de Neurologie, INSERM UMR 975 Centre de Recherche de l'Institut du Cerveau et la Moelle Epinière (CRICM), Université Pierre et Marie Curie (UPMC), Pitié-Salpêtrière, Paris, France. <sup>19</sup>Department of Neurology, Klinikum Rechts der Isar, Technische Universität München, Munich, Germany. <sup>20</sup>Munich Cluster for Systems Neurology (SyNergy), Munich, Germany. <sup>21</sup>German Competence Network Multiple Sclerosis (KKNMS), Munich, Germany. <sup>22</sup>Department of Clinical Sciences, Danderyd Hospital, Karolinska Institutet, Stockholm, Sweden. <sup>23</sup>Focus Program Translational Neuroscience (FTN), Rhine Main Neuroscience Network (rmn2), Johannes Gutenberg University Medical Center, Mainz, Germany. <sup>24</sup>Department of Health Sciences, University of Eastern Piedmont, Novara, Italy. <sup>25</sup>Interdisciplinary Research Center of Autoimmune Diseases (IRCAD), University of Eastern Piedmont, Novara, Italy. <sup>26</sup>Laboratory of Genetics of Neurological Complex Disorders, Institute of Experimental Neurology (INSPE), Division of Neuroscience, San Raffaele

Scientific Institute, Milan, Italy. <sup>27</sup>Department of Neurology, INSPE, Division of Neuroscience, San Raffaele Scientific Institute, Milan, Italy. <sup>28</sup>Menzies Research Institute Tasmania, University of Tasmania, Hobart, Tasmania, Australia. <sup>29</sup>Department of Neurology, Oslo University Hospital, Ullevål, Oslo, Norway. <sup>30</sup>University of Oslo, Oslo, Norway. <sup>31</sup>Department of Neuroscience, Karolinska Institutet, Stockholm, Sweden. <sup>32</sup>Department of Neurology, University of California, San Francisco, Sandler Neurosciences Center, San Francisco, California, USA. <sup>33</sup>Department of Neurology, Erasmus MC, Erasmus University Medical Centre, Rotterdam, The Netherlands. <sup>34</sup>Division of Epidemiology, Genetic Epidemiology and Genomics Laboratory, School of Public Health, University of California, Berkeley, Berkeley, California, USA. <sup>35</sup>California Institute for Quantitative Biosciences (QB3), University of California, Berkeley, Berkeley, California, USA. <sup>36</sup>Kaiser Permanente Division of Research, Oakland, California, USA. <sup>37</sup>Full lists of members and affiliations appear in the **Supplementary Note**. <sup>38</sup>Laboratory of Molecular Medicine and Biotechnology, Don C. Gnocchi Foundation Organizzazione Non Lucrativa di Utilità Sociale (ONLUS), Istituto di Ricovero e Cura a Carattere Scientifico (IRCCS) Santa Maria Nascente, Milan, Italy. <sup>39</sup>Institute of Environmental Medicine, Karolinska Institutet, Stockholm, Sweden. <sup>40</sup>Laboratoire d'Immunologie, Université Rennes 1, Rennes, France. <sup>41</sup>Medical Research Council Biostatistics Unit, Cambridge, UK. <sup>42</sup>Department of Transfusion Medicine, University Medical Center Hamburg-Eppendorf, Hamburg, Germany. <sup>43</sup>School of Medicine, Griffith University, Gold Coast, Queensland, Australia. <sup>44</sup>Centre Hospitalier Universitaire (CHU) Pellegrin, Université Bordeaux 2, Bordeaux, France. <sup>45</sup>Department of Medicine, University of Melbourne, Melbourne, Victoria, Australia. <sup>46</sup>Department of Neurology, Box Hill Hospital, Monash University, Box Hill, Victoria, Australia. <sup>47</sup>Service de Neurologie, Centre Hospitalier Universitaire Régional Montpellier, Montpellier, France. <sup>48</sup>Plateforme Post-Génomique P3S, Université Pierre et Marie Curie, INSERM, Paris, France. <sup>49</sup>Department of Neuroscience, Multiple Sclerosis Center, Azienda Ospedaliera Città della Salute e della Scienza di Torino, Turin, Italy. <sup>50</sup>Department of Neuroscience, University of Turin, Turin, Italy. <sup>51</sup>Service de Neurologie, Hôpital Avicenne, Bobigny, France. <sup>52</sup>Department of Health Sciences, San Paolo Hospital and Filarete Foundation, University of Milan, Milan, Italy. <sup>53</sup>Service de Neurologie, CHU de Caen and INSERM U919–Groupement d'Intérêt Public Cyceron, Caen, France. <sup>54</sup>Department of Neurology, Multiple Sclerosis Division, Miller School of Medicine, University of Miami, Miami, Florida, USA. <sup>55</sup>Neurologia 2–Regional Multiple Sclerosis Centre, Azienda Ospedaliera Universitaria San Luigi, Orbassano, Turin, Italy. <sup>56</sup>Department of Neurology, Royal Victoria Infirmary, Newcastle-upon-Tyne, UK. <sup>57</sup>Department of Neurology, University of Tampere, Medical School, Tampere, Finland. <sup>58</sup>Division of Clinical Neurology, Nottingham University Hospital, Nottingham, UK. <sup>59</sup>Florey Institute of Neuroscience and Mental Health, University of Melbourne, Melbourne, Victoria, Australia. <sup>60</sup>Institute of Clinical Molecular Biology, Christian Albrechts University of Kiel, Kiel, Germany. <sup>61</sup>Department of Pathophysiology and Transplantation, Neurology Unit, University of Milan, Milan, Italy. <sup>62</sup>Fondazione IRCCS Cà Granda Ospedale Maggiore Policlinico, Milan, Italy. <sup>63</sup>Kora-gen, Helmholtz Zentrum München–German Research Center for Environmental Health, Institute of Genetic Epidemiology, Neuherberg, Germany. <sup>64</sup>Department of Clinical Neurology, The Ipswich Hospital National Health Service (NHS) Trust, Ipswich, UK. <sup>65</sup>Center for Applied Genomics, The Children's Hospital of Philadelphia, Philadelphia, Pennsylvania, USA. <sup>66</sup>Department of Pediatrics, The Perelman School of Medicine, University of Pennsylvania, Philadelphia, Pennsylvania, USA. <sup>67</sup>Wellcome Trust Clinical Research Facility, Southampton General Hospital, Southampton, UK. <sup>68</sup>Department of Neurology, Aberdeen Royal Infirmary, Aberdeen, UK. <sup>69</sup>Department of Medical Epidemiology and Biostatistics, Karolinska Institutet, Stockholm, Sweden. <sup>70</sup>Department of Medicine at Karolinska University Hospital Solna, Atherosclerosis Research Unit, Center for Molecular Medicine, Karolinska Institutet, Stockholm, Sweden. <sup>71</sup>Department of Neurology, Hull Royal Infirmary, Hull, UK. <sup>72</sup>Department of Neurology, Royal Devon and Exeter Foundation Trust Hospital, Exeter, UK. <sup>73</sup>Keele University Medical School, University Hospital of North Staffordshire, Stoke-on-Trent, UK. <sup>74</sup>UCL Genetics Institute (UGI), University College London, London, UK. <sup>75</sup>Department of Neurology, Poole General Hospital, Poole, UK. <sup>76</sup>Plymouth University Peninsula Schools of Medicine and Dentistry, Plymouth, UK. <sup>77</sup>Institute for Neuroimmunology and Clinical Multiple Sclerosis Research (inims), Center for Molecular Neurobiology (ZMNH), University Medical Center Hamburg-Eppendorf, Hamburg, Germany. <sup>78</sup>Department of Neuroimmunology and Multiple Sclerosis Research, Neurology Clinic, University Hospital Zürich, Zürich, Switzerland. <sup>79</sup>Department of Neurology, Division of Clinical Neurology, Leicester Royal Infirmary, Leicester, UK. <sup>80</sup>Australian Neuromuscular Research Institute, University of Western Australia, Nedlands, Western Australia, Australia. <sup>81</sup>Institute for Immunology and Infectious Diseases, Murdoch University, Murdoch, Western Australia, Australia. <sup>82</sup>Melbourne Neuroscience Institute, University of Melbourne, Melbourne, Victoria, Australia. <sup>83</sup>Department of Neurology, Seinäjoki Central Hospital, Seinäjoki, Finland. <sup>84</sup>Department of Physics, Chemistry and Biology (IFM) Bioinformatics, Linköping University, Linköping, Sweden. <sup>85</sup>Fondation Jean Dausset–Centre d'Etude du Polymorphisme Humain, Paris, France. <sup>86</sup>Commissariat à l'Energie Atomique, Institut Génomique, Centre National de Génotypage, Evry, France. <sup>87</sup>McGill University and Génomique Québec Innovation Centre, Montreal, Quebec, Canada. <sup>88</sup>Service de Neurologie, Hôpital Pasteur, CHRU Nice, France. <sup>89</sup>Hunter Medical Research Institute, University of Newcastle, Newcastle, New South Wales, Australia. <sup>90</sup>Department of Neurology, Ospedale Maggiore, Novara, Italy. <sup>91</sup>Department of Medical Genetics, Oslo University Hospital, Ullevål, Oslo, Norway. <sup>92</sup>Department of Vertebrate Genomics, Neuropsychiatric Genetics Group, Max Planck Institute for Molecular Genetics, Berlin, Germany. <sup>93</sup>Department of Clinical Neurosciences and Rehabilitation, Institute of Neuroscience and Physiology, Sahlgrenska Academy, Göteborgs Universitet, Göteborg, Sweden. <sup>94</sup>Department of Psychiatry and Human Behavior, School of Medicine, University of California–Irvine, Irvine, California, USA. <sup>95</sup>Department of Pharmacological and Biomolecular Sciences, University of Milan, Milan, Italy. <sup>96</sup>Department of Chronic Disease Prevention, National Institute for Health and Welfare, Helsinki, Finland. <sup>97</sup>Canterbury District Health Board, Christchurch, New Zealand. <sup>98</sup>Department of Neurology, Queen Elizabeth Medical Centre, Edgbaston, Birmingham, UK. <sup>99</sup>Department of Neurology, The Norwegian Multiple Sclerosis Registry and Biobank, Haukeland University Hospital, Bergen, Norway. <sup>100</sup>National Multiple Sclerosis Center Melsbroek, Melsbroek, Belgium. <sup>101</sup>Neurology Department, Charing Cross Hospital, London, UK. <sup>102</sup>Department of Clinical Sciences, Lund University, Lund, Sweden. <sup>103</sup>Department of Neurology, Royal Hallamshire Hospital, Sheffield, UK. <sup>104</sup>Department of Neurology, University of Oulu, Oulu, Finland. <sup>105</sup>Department of Neurology, University Hospital of Oulu, Oulu, Finland. <sup>106</sup>Laboratory of Neurobiology, Vesalius Research Center, Leuven, Belgium. <sup>107</sup>Experimental Neurology, Leuven Research Institute for Neurodegenerative Diseases (LIND), University of Leuven (KU Leuven), Leuven, Belgium. <sup>108</sup>Department of Neurology, University Hospitals Leuven, Leuven, Belgium. <sup>109</sup>Institute of Psychological Medicine and Clinical Neuroscience, Cardiff University, University Hospital of Wales, Cardiff, UK. <sup>110</sup>Department of Neurology, Greater Manchester Neurosciences Centre, Salford Royal NHS Foundation Trust, Salford, UK. <sup>111</sup>Department of Neuroscience, Centre for Experimental Neurological Therapies, Mental Health and Sensory Organs, Sapienza Università di Roma, Rome, Italy. <sup>112</sup>Department of Neurology, Royal Preston Hospital, Preston, UK. <sup>113</sup>Department of Neurology, Norfolk and Norwich Hospital, Norwich, UK. <sup>114</sup>Department of Neurology, Flinders University, Adelaide, South Australia, Australia. <sup>115</sup>Institute of Basic Medical Sciences, University of Oslo, Oslo, Norway. <sup>116</sup>Department of Neurology, Peterborough City Hospital, Peterborough, UK. <sup>117</sup>Neurology and Stroke Unit, San Francesco Hospital, Nuoro, Italy. <sup>118</sup>Department of Neurology, Helsinki University Central Hospital and Molecular Neurology Programme, Biomedicum, University of Helsinki, Helsinki, Finland. <sup>119</sup>Department of Epidemiology, Erasmus Medical Center, Rotterdam, The Netherlands. <sup>120</sup>Division of Applied Health Sciences, University of Aberdeen, Foresterhill, Aberdeen, UK. <sup>121</sup>Institute of Clinical Neurosciences, University of Bristol, Frenchay Hospital, Bristol, UK. <sup>122</sup>Centre for Population Health Sciences, University of Edinburgh, Edinburgh, UK. <sup>123</sup>Institut für Humangenetik, Technische Universität München, Munich, Germany. <sup>124</sup>Institut für Humangenetik, Helmholtz Zentrum München–Munich, Germany. <sup>125</sup>Harvard NeuroDiscovery Center, Harvard Medical School, Boston, Massachusetts, USA. <sup>126</sup>Department of Immunobiology, Yale University School of Medicine, New Haven, Connecticut, USA. <sup>127</sup>These authors contributed equally to this work. <sup>128</sup>These authors jointly directed this work. Correspondence should be addressed to J.L.M. ([jmccauley@med.miami.edu](mailto:jmccauley@med.miami.edu)).



## ONLINE METHODS

**ImmunoChip data (discovery set).** Details of case ascertainment, processing and genotyping for the discovery phase are provided in the **Supplementary Note** (see also **Supplementary Table 9**). All cases and controls involved in this study gave valid informed consent in accordance with approval from the relevant local ethical committees or institutional review boards (IRBs). The investigators were not blinded to allocation during experiments and outcome assessment. Genotype calling for all samples was performed using Optical<sup>40</sup>. Samples that performed poorly or were determined to be related were removed (**Supplementary Table 10**). Data were organized into 11 country-level strata: ANZ (Australia and New Zealand), Belgium, Denmark, Finland, France, Germany, Italy, Norway, Sweden, the UK and the United States. SNP-level quality control (**Supplementary Table 11**) and population outlier identification using principal-components analysis (**Supplementary Fig. 97**) were carried out in each stratum separately. No statistical method was used to pre-determine sample size.

**Discovery set analysis.** We applied logistic regression, assuming a per-allelic genetic model for each data set, including the first five principal components as covariates to correct for population stratification (**Supplementary Table 12** lists the genomic inflation factors for each data set,  $\lambda$ ). We then performed an inverse variance meta-analysis of the 11 strata under a fixed-effects model, as implemented in PLINK<sup>41</sup>. To be more conservative and account for any residual inflation in the test statistic, we applied the genomic control equivalent to the per-SNP standard error in each stratum. Specifically, we corrected the standard errors for SNPs by multiplying them by the square root of the raw genomic inflation factor,  $\lambda$ , for each data set if  $\lambda$  was  $>1$ .

Within the designated fine-mapping intervals, we applied a forward stepwise logistic regression to identify statistically independent effects. The primary SNP in each interval was included as a covariate, and association analysis was repeated for the remaining SNPs. This process was repeated until no SNPs reached the minimum level of significance ( $P < 1 \times 10^{-4}$ ). Outside of the designated fine-mapping intervals, all SNPs having association  $P < 1 \times 10^{-4}$  were identified and grouped into sets on the basis of being separated by a physical distance of less than 2 Mb, and a similar stepwise regression model was applied. Any SNPs that entered the model with association  $P < 1 \times 10^{-4}$  after conditioning were considered to be statistically independent primary signals.

In addition, because of the close physical proximity of some fine-mapping intervals and SNP sets, independence was tested for all identified signals within 2 Mb of one another. Forest and cluster plots (**Supplementary Fig. 98**) of all independent SNPs were examined, and a SNP was excluded if cluster plots were unsatisfactory. If a SNP was excluded, forward stepwise logistic regression within the corresponding fine-mapping interval or SNP set was repeated after removal of the SNP. During this process, 17 additional SNPs were excluded on the basis of cluster or forest plot review.

**Replication set.** The replication phase included GWAS data organized into 15 strata. Within each stratum, poorly performing samples (call rate  $< 95\%$ , sex discordance or excess heterozygosity) and poorly performing SNPs (Hardy-Weinberg equilibrium  $P < 1 \times 10^{-6}$ , minor allele frequency (MAF)  $< 1\%$  or call rate  $< 95\%$ ) were removed. Principal-components analysis was performed to identify population outliers for each stratum, and the genomic control inflation factor was  $< 1.1$  for each. Data included in the final discovery and replication analyses are summarized in **Supplementary Tables 13** and **14**. All samples used in the replication set were unrelated to those in the discovery set, as verified by identity-by-descent analysis.

We attempted replication of all non-MHC independent signals that reached discovery  $P < 1 \times 10^{-4}$  in a meta-analysis set of GWAS. Each data set was imputed with the 1000 Genomes Project European phase I (a) panel using BEAGLE<sup>42</sup> to maximize the overlap between the ImmunoChip SNP content and the GWAS data. Post-imputation genotypic probabilities were used in a logistic regression model, for each stratum, to estimate SNP effect sizes and  $P$  values. By using the post-imputation genotypic probabilities, we penalized SNPs that did not have good imputation quality, thus ensuring a conservative analysis. Furthermore, we accounted for population stratification in each data set by including the first five principal components in the logistic model.

We then performed meta-analysis of the effect sizes and respective standard errors of the 15 strata using a fixed-effects, inverse variance method. We applied the genomic control equivalent to the per-SNP standard error in each stratum, controlling for the respective genomic inflation factor,  $\lambda$  (**Supplementary Table 14**).

To replicate the primary SNPs with identified signal in the discovery phase, we determined the replication effect sizes and respective standard errors. For the secondary and tertiary SNPs, we fitted the same exact models as in the discovery phase for each data set. We then performed fixed-effects meta-analysis to estimate an effect size that corresponded to the same logistic model. In the case that a SNP was not present in the replication set, we replaced it with a perfectly tagging SNP, i.e., a SNP that had  $r^2$  and  $D'$  values equal to 1. If a perfectly tagging SNP was not available, we selected a SNP that had equivalent MAF and the highest possible  $r^2$  and  $D'$  values. Estimation of  $r^2$  and  $D'$  values for this objective were based on data from ImmunoChip control samples.

**Joint analysis (discovery and replication sets).** We performed meta-analysis of the effect sizes and respective standard errors from the discovery and replication phases under a fixed-effects model. A SNP was considered to have replicated when all three of the following criteria were met: (i) replication  $P < 5.0 \times 10^{-2}$ ; (ii) joint  $P < 5 \times 10^{-8}$ ; and (iii) the joint  $P$  value was more statistically significant than the discovery  $P$  value. SNPs that reached  $P < 1 \times 10^{-6}$  but did not pass the genome-wide significance threshold were defined as having suggestive signals if criteria (i) and (iii) were met.

**Fine mapping of association signals.** To fine map association signals, we used a combination of imputation and Bayesian methodology<sup>23</sup>. Around each of the 97 associated SNPs, we isolated 2 Mb of sequence in the discovery and replication phase UK data as well as in the European samples from Phase 1 of the 1000 Genomes Project<sup>28</sup>. Forming the single largest cohort, only UK samples were considered to minimize the effects of differential imputation quality between populations of different ancestry. In addition to the previous quality control, SNPs with failed alignment or difference in MAF  $> 10\%$  between the typed cohorts and the 1000 Genomes Project samples, MAF  $< 1\%$  or Hardy-Weinberg equilibrium  $P < 1.0 \times 10^{-4}$  were removed.

Imputation was performed separately for the UK discovery and replication cohorts on each 2-Mb region using the default settings of IMPUTEv2 (refs. 43,44). Missing genotypes for the genotyped SNPs were not imputed, and any imputed SNP that failed to reach the Hardy-Weinberg equilibrium and MAF thresholds was subsequently removed. We carried out frequentist and Bayesian association tests on all SNPs in each cohort separately, assuming additivity, using the default settings of SNPTESTv2 (ref. 45). Frequentist fixed-effects meta-analysis was carried out using the software META<sup>46</sup>. Bayesian meta-analysis was carried out using an independence prior (near-identical results were obtained using a fixed-effects Bayesian meta-analysis).

To identify regions where reliable fine mapping could be achieved, we used the information score (INFO, obtained from IMPUTEv2) as determined from the 1000 Genomes Project samples. Specifically, we measured the fraction of variants having both  $r^2 > 0.5$  and  $r^2 > 0.8$  with the primary associated variant and having greater than 50% and 80% INFO scores, respectively. Regions where any SNP with  $r^2 > 0.5$  had INFO  $< 50\%$  were excluded. We also excluded regions where the top hit from imputation had an INFO score less than 80%. Regions were considered to be fine mapped with high quality when all variants with  $r^2 > 0.8$  had an INFO score of at least 80%. Within these regions, we excluded variants where the inferred direction of association was opposite between the UK discovery and replication cohorts.

To measure the posterior probability that any single variant drives association, we calculated the Bayes factor. Under the assumption that there is a single causal variant in the region, the Bayes factor is proportional to the probability that the variant drives the association<sup>23</sup>. We identified the smallest set of variants that contained 90% and 50% of the posterior probability. We called a region successfully and consistently fine mapped if it there were at most five variants in the 50% confidence interval and the top SNP from the frequentist analysis was contained in the 90% confidence interval. For these regions, we annotated variants with information about evolutionary conservation, predicted coding consequences, regulation, published associations to expression

or DNase I hypersensitive sites using ANNOVAR<sup>47</sup>, VEP<sup>24</sup> and the eQTL browser, a recent study of expression in immune cells<sup>20</sup> and other literature.

**GO classification.** To determine the GO processes in which our 97 associated variants were involved, we used MetaCore from Thomson Reuters. We annotated the processes for the unique genes within 50 kb of the variants.

**Cross-disease comparisons.** To explore the potential overlap with variants identified across other autoimmune diseases, we calculated the percentage overlap of reported variants found in other ImmunoChip reports to our ImmunoChip results. The top variants reported as either newly discovered or previously known in other ImmunoChip reports were compared with the 110 variants representing both our new and previous discoveries in multiple sclerosis. For a signal to be considered to be overlapping, we required  $r^2 \geq 0.8$  using the Pairwise LD function of the SNAP tool in European samples<sup>31</sup>.

**Secondary analyses.** We performed a severity-based analysis of the Multiple Sclerosis Severity Score (MSSS) in cases only from the discovery phase

(**Supplementary Fig. 99**). In addition, a transmission disequilibrium test was performed in 633 trios to test for transmission of the 97 identified risk alleles (**Supplementary Fig. 100**). Details are given in the **Supplementary Note**.

40. Shah, T.S. *et al.* optiCall: a robust genotype-calling algorithm for rare, low-frequency and common variants. *Bioinformatics* **28**, 1598–1603 (2012).
41. Purcell, S. *et al.* PLINK: a tool set for whole-genome association and population-based linkage analyses. *Am. J. Hum. Genet.* **81**, 559–575 (2007).
42. Browning, B.L. & Yu, Z. Simultaneous genotype calling and haplotype phasing improves genotype accuracy and reduces false-positive associations for genome-wide association studies. *Am. J. Hum. Genet.* **85**, 847–861 (2009).
43. Marchini, J., Howie, B., Myers, S., McVean, G. & Donnelly, P. A new multipoint method for genome-wide association studies by imputation of genotypes. *Nat. Genet.* **39**, 906–913 (2007).
44. Howie, B., Marchini, J. & Stephens, M. Genotype imputation with thousands of genomes. *G3* **1**, 457–470 (2011).
45. Marchini, J. & Howie, B. Genotype imputation for genome-wide association studies. *Nat. Rev. Genet.* **11**, 499–511 (2010).
46. Liu, J.Z. *et al.* Meta-analysis and imputation refines the association of 15q25 with smoking quantity. *Nat. Genet.* **42**, 436–440 (2010).
47. Wang, K., Li, M. & Hakonarson, H. ANNOVAR: functional annotation of genetic variants from high-throughput sequencing data. *Nucleic Acids Res.* **38**, e164 (2010).